

Learning Feature-Preserving Portrait Editing from Generated Pairs

Bowei Chen^{1*} Tiancheng Zhi² Peihao Zhu² Shen Sang² Jing Liu² Linjie Luo²
¹ University of Washington, ² ByteDance
 boweiche@cs.washington.edu,
 {tiancheng.zhi, peihao.zhu, shen.sang, jing.liu, linjie.luo}@bytedance.com



Figure 1. Our method takes a portrait image as input, and applies advanced editing effects with our proposed framework. We can handle both real human portraits (1st row) as well as cartoon characters (2nd row). Our approach obtains superior aesthetic quality while at the same time preserving key features from the input subject. Compared with baseline approaches (left), we achieve better subject feature preservation (e.g., identity), structural alignment, and fewer artifacts.

Abstract

Portrait editing is challenging for existing techniques due to difficulties in preserving subject features like identity. In this paper, we propose a training-based method leveraging auto-generated paired data to learn desired editing while ensuring the preservation of unchanged subject features. Specifically, we design a data generation process to create reasonably good training pairs for desired editing at low cost. Based on these pairs, we introduce a Multi-Conditioned Diffusion Model to effectively learn the editing direction and preserve subject features. During inference, our model produces accurate editing mask that can guide the inference process to further preserve detailed subject

features. Experiments on costume editing and cartoon expression editing show that our method achieves state-of-the-art quality, quantitatively and qualitatively.

1. Introduction

Portrait editing is increasingly favored in photo and social applications. In many of these applications, users can select from a set of pre-defined editing options and then apply their chosen edits to their own photos. In practice, the key requirement of portrait editing is to deliver outcomes that achieve selected editing while *strictly* preserving the features of subjects intended to remain unaltered (e.g., identity and clothing for expression editing). Nevertheless, meeting this requirement poses a considerable challenge, as even

*Work done during internship at ByteDance.

slight deviations in these features can markedly affect the perceived quality of the outcome. Therefore, the goal of this paper is to design a portrait editing pipeline that can achieve superior editing outcomes for a specific editing task favored by users.

Existing image editing approaches fail to satisfy the requirements of portrait editing tasks. They can be categorized into two types. The first one is training-free methods, which mainly rely on a pretrained diffusion model [39] to perform editing guided by a text prompt. However, they suffer from two limitations. (1) They struggle to achieve desired editing as they depend on inversion techniques to reverse the input image into a denoising process, which may hurt editability. (2) They fail to preserve detailed subject features as little prior knowledge for invariance is enforced. Figure 1 (left) shows outputs of a training-free method Prompt2Prompt [19]. Another stream of work is training-based methods, aiming to learn the editing direction for desired changes, and also preserve untargeted subject features, with a training set. However, these methods require extremely high-quality training dataset, which is usually hard to collect. Figure 1 (left) shows outputs of a recent training-based method BBDM [26].

In this paper, we opt for training using a synthetic dataset generated automatically at low cost, thereby eliminating the necessity of manually collecting datasets. Our framework generates a synthetic dataset for any user-defined editings and uses this dataset to effectively learn the editing directions, fulfilling the aforementioned requirements, and upholding high image quality. Specifically, we first design a conditional dataset generation strategy to produce diverse paired data given text prompts, which has better identity and layout alignment than existing data generation strategy. Given these pairs, we design a Multi-Conditioned Diffusion Model (MCDM) to effectively learn editing direction and preserve the subject features. This is achieved by injecting the conditional signals from input image and text prompt into the diffusion model through different ways. Finally, we demonstrate that the trained MCDM can *explicitly* identify regions expected to change (*e.g.*, face regions for expression editing), producing an editing mask. This provides guidance for our inference process to further keep subject features untouched.

As shown in Figure 1, our editing results achieve expressive styles while preserving subject features, in both real person costume and cartoon expression editing cases. The effectiveness of the method is further validated through comprehensive quantitative analysis and user studies, which collectively demonstrate its clear superiority over existing baseline methods.

Contributions: (1) A data generation technique providing paired data with better identity and layout alignment; (2) A Multi-Conditioned Diffusion Model producing feature-

preserving results and accurate editing masks for inference guidance; (3) State-of-the-art portrait editing results.

2. Related Work

Image generation and editing have seen significant advancements with generative models like GANs [17], VAEs [25], and normalizing flows [37], leading to highly realistic outputs [23, 24]. Recent breakthroughs in diffusion models [21, 46–48], such as Imagen [43], GLIDE [32], DALL-E2 [36], and Stable Diffusion [39], have further revolutionized this field. They can generate a wide variety of images from mere textual descriptions and has spurred research into their applications in image editing.

Training-Free Approaches: Prevalent editing methods rely on inverting images into a model’s latent space [1, 2, 50, 52, 53] and editing by manipulating latent codes [2, 18, 44] or model weights [3, 6, 15, 38], without new model training. They are known as training-free methods. Text-to-image diffusion models, akin to GANs, use Gaussian noise as latent input, combined with textual guidance, to generate images. Methods like SDEdit [28] add noise to the input image for a fixed number of steps, and then initiate a text-guided denoising process for repainting. However, these methods apply global editing, failing to preserve details in areas not targeted for modification. To overcome this issue, some studies [4, 5, 31] use user-provided masks to define editing regions, thus allowing for partial edits. Yet, obtaining precise masks for editing is non-trivial, and mask-based inpainting methods often result in the loss of image information within the masked area, disrupting the consistency between the pre- and post-edit images.

For controlled, local editing, Prompt2Prompt [19] and DiffEdit [11] have been developed. The former preserves layout and subject geometry through cross-attention maps, while the latter generates an editing mask through contrasting predictions from different text conditions. Both methods employ DDIM inversion [14, 47] to encode input images. However, DDIM inversion, especially with classifier-free guidance, often leads to unsatisfactory reconstruction and editing outcomes. Null-text Inversion [29] improves inversion reconstruction while retaining the editing capabilities. Pix2pix-zero [34] improves DDIM inversion through noise regularization [24] and introduces cross-attention loss during the denoising process. However, this method may pose difficulties in terms of control and could lead to unexpected outcomes, especially for portrait editing.

Training-Based Approaches: Training-based methods learn editing direction from a large dataset. Li et al. [26] and Sheynin et al. [45] train diffusion models for image-to-image translation and local semantic editing without inversion, but their expressiveness and quality lag behind current large-scale diffusion models. InstructPix2Pix [7] uses GPT-3 [9] and Prompt2Prompt [19] to create text edited pairs and

distills a diffusion model, generally producing more controlled edits and showing robustness with real image inputs. The effectiveness of training-based methods depends on the quality of the constructed pairs. Our method, which falls into this category, achieves greater consistency and superior editing results by using Composable Diffusion [27] to generate better pairs. Relying on our condition injection mechanism and network design, we are capable of producing edits which are less affected by data imperfection, and thus better preserving input features.

Diffusion-based editing also relates to concept embedding [16], model fine-tuning [41], and controlled generation [30, 51], but they are outside our discussion scope.

3. Our Pipeline

Given an input portrait image x_A in the source domain A , our goal is to synthesize a high-quality portrait image \hat{x}_B in domain B . A well-edited image \hat{x}_B should: (1) retain the untargeted subject features (e.g., identity) and rough layout from x_A , (2) ensure editing fidelity (i.e., $\hat{x}_B \in B$) and maintain high image quality.

To this end, we design a diffusion-based image editing pipeline with three stages. (1) We first introduce an automated data generation strategy to create reasonably good but not perfect pairs of input x_A and ground truth x_B (Figure 2 left). (2) Then we design and train a Multi-Conditioned Diffusion Model (MCDM) (Figure 2 right) on this generated dataset. By leveraging multiple conditions in different ways, MCDM can effectively learn the editing direction from the training pairs, while preserving detailed subject features that are not supposed to be changed. (3) During inference, we generate edited results using the trained MCDM with an automatically generated editing mask to further preserve subject details in x_A .

3.1. Preliminary

We start with a quick overview of Latent Diffusion [39] and establish notations that we use throughout. Latent Diffusion has two components: (1) a Variational Autoencoder, including an encoder E to transform an image x into a latent code $z = E(x)$, and a decoder D to map z back to an image $x' = D(z)$, (2) a U-Net $\epsilon_\theta(z_t, t, C)$ which predicts added noise given a noisy latent. z_t is the noisy latent code at timestep t and C is a *tuple* of conditional signals.

To generate an image, a noisy latent z_T is randomly sampled and processed through denoising by the U-Net over a fixed number of timesteps, denoted as T . The iterative denoising process transforms z_T into a clean latent z_0 , which is subsequently utilized by the decoder D to generate the image. Specifically, at timestep t , the denoised latent z_{t-1} is sampled based on z_t and $\tilde{\epsilon}_\theta(z_t, t, C)$, which is computed using classifier-free guidance [20]. Here is an example with

two elements in C , given by:

$$\begin{aligned} \tilde{\epsilon}_\theta(z_t, t, C) = & \epsilon_\theta(z_t, t, \{\emptyset, \emptyset\}) \\ & + s_1(\epsilon_\theta(z_t, t, \{c_1, \emptyset\}) - \epsilon_\theta(z_t, t, \{\emptyset, \emptyset\})) \\ & + s_2(\epsilon_\theta(z_t, t, \{c_1, c_2\}) - \epsilon_\theta(z_t, t, \{c_1, \emptyset\})), \end{aligned} \quad (1)$$

where c_1 and c_2 denote two conditional signals, with \emptyset representing a null value (e.g., a black image for image condition). s_1 and s_2 are the weights for c_1 and c_2 , respectively. Eq. 1 can also be easily rewritten to suit the case of one or three conditional signals.

For clarity, we primarily use the task of costume editing to illustrate the pipeline. The goal is to transform a person with a regular outfit into a Santa Claus costume.

3.2. Paired Data Generation

The goal is to design a data generation strategy that can produce paired exemplars aligned with a specified editing direction (e.g., from regular to Santa Claus costumes) defined by text prompts. However, generating pairs with perfect spatial and identity alignment is very challenging. Thus we seek to design a strategy (Figure 2 left) that can generate reasonably good pairs, meeting these essential criteria: (1) the user identity in input x_A and ground truth x_B should match as closely as possible; (2) x_A and x_B should have rough spatial alignment; (3) the data should cover a diverse range of user appearances (for better generalization).

One straightforward idea suggested by Instruct-Pix2Pix [8] is to use GPT-3 [9] for generating a pair of text prompts in the source and target domains. These generated prompts are then employed to create x_A and x_B using a pretrained Stable Diffusion model [39] and the Prompt2Prompt image editing technique [19]. However, this method often results in unsatisfactory x_B as it fails to preserve the identity in x_A , as depicted in Figure 3 (a).

Instead, we build a conditional pair generation strategy on top of Composable Diffusion [27] to meet the three requirements. Key designs include: (1) Following [27], we generate x_A and x_B within a single image achieved through a single denoising process. This helps generate consistent identities in x_A and x_B (criterion 1). (2) We incorporate pose information to improve spatial alignment (criterion 2). (3) We extract identity information from real photos and use this information to ensure criterion 1 and 3.

To implement design (1), we employ a pretrained Stable Diffusion in conjunction with Composable Diffusion [27] to generate an image $x = [x_A, x_B] \in \mathbb{R}^{H \times 2W \times 3}$, where the operator $[\cdot, \cdot]$ represents the horizontal concatenation of two images. Here, H and W denote the height and width of x_A and x_B . Further, the design (2) and (3) are implemented as conditions to guide the denoising process of x .

Specifically, we begin by randomly initializing a latent code $z_T \in \mathbb{R}^{h \times 2w \times 4}$, where $h = H/8$, $w = W/8$, and 4

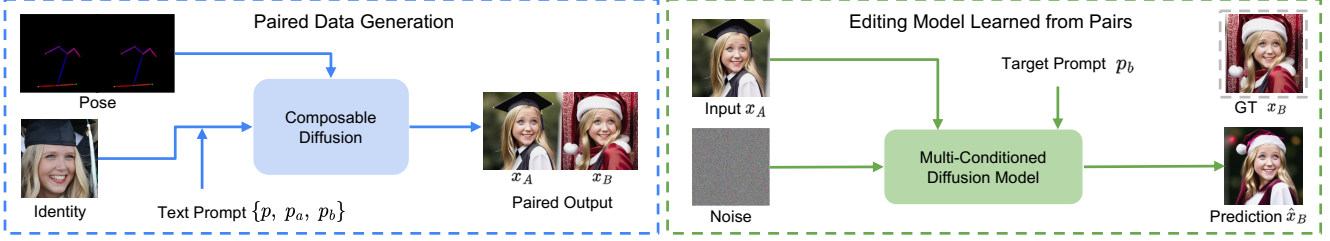


Figure 2. Overview of our pipeline. *Paired Data Generation* (blue dashed box) first constructs training pairs using Composable Diffusion [27] conditioning on pose and identity information. *Multi-Conditioned Diffusion Model* (green dashed box) encodes multiple condition signals to learn the editing direction and preserve subject features based on the generated pairs. The multi-condition design enhances the robustness in handling imperfections within training pairs.



Figure 3. Examples of pairs generated by different strategies. Prompt-to-Prompt (a) fails to produce pairs with consistent identity. Without pose condition, (b) produces pairs with significant spatial misalignment. Without identity conditions, (c) results in pairs with obvious face shapes difference. Our strategy (d) significantly improves these issues.

represents the feature dimension of the latent code. At each timestep t , we compute the predicted noise by combining three classifier-free guidance results:

$$\begin{aligned} \bar{\epsilon} = & s'_d \cdot \tilde{\epsilon}_{\theta'}(z_t, t, \{c_p, c_{id}\}) + \\ & s'_a \cdot M'_a \odot \tilde{\epsilon}_{\theta'}(z_t, t, \{c_{p_a}, c_{id}\}) + \\ & s'_b \cdot M'_b \odot \tilde{\epsilon}_{\theta'}(z_t, t, \{c_{p_b}, c_{id}\}), \end{aligned} \quad (2)$$

where c_p , c_{p_a} , and c_{p_b} represent text embeddings computed from the shared prompt p , the source prompt p_a , and the target prompt p_b , respectively. In the example of Figure 2, p is “the same woman on the left and right”, p_a is “a woman, normal costume”, and p_b is “a woman, santa claus costume”. c_{id} denotes identity embeddings (design (3)) extracted from a real-world portrait image using a variant of CLIP-based identity encoder [49], trained on the FFHQ dataset [23]. This encoder translates an image into multiple textual word embeddings, thus can be combined with c_p ,

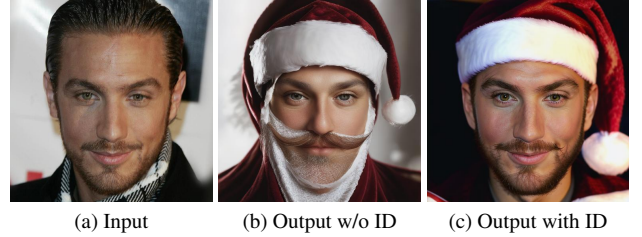


Figure 4. Training on a dataset with less diverse identities (b) results in inconsistent identity with the input (a). Conversely, training on a dataset with diverse identities yields the desired editing outcome (c), demonstrating its better generalization ability.

c_{p_a} , and c_{p_b} to provide identity information for the denoising process. See supplementary for further details.

The matrices M'_a and M'_b are defined as $[1, 0]$ and $[0, 1]$ respectively, both belonging to $\mathbb{R}^{h \times 2w \times 4}$. Here, $\mathbf{1}$ ($\mathbf{0}$) represents a matrix in the dimension $h \times w \times 4$ with all values set to one (zero). Additionally, the variables s'_d , s'_a , and s'_b signify the strengths associated with each predicted noise. Furthermore, the denoising process is guided by a pose image (design (2)) using the OpenPose [10] ControlNet [51], as shown in Figure 2 top left. This pose image ensures alignment by featuring the same pose in both the left and right parts of the image. The pair generated by our approach is depicted in Figure 2 on the left.

Notably, both design (2) (for pose) and design (3) (for identity) play a crucial role in generating good pairs. Figure 3 illustrates this point. Dropping one of them results in considerable spatial misalignment (b) and noticeable differences in facial shape (c). In addition, design (3) also contributes to generating diverse individuals across different pairs. This is crucial for enhancing generalization ability, as shown in Figure 4.

3.3. Training Multi-Conditioned Diffusion Model

Although the generated pairs are reasonably good, they are still not perfect. For example, in Figure 2, the face in x_B is

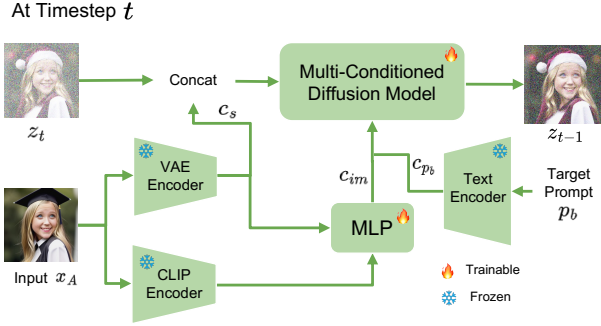


Figure 5. Illustration of Multi-Conditioned Diffusion Model, where both image and text embeddings are injected into the model through different ways to effectively learn the editing direction and preserve subject features.

slightly wider than that in x_A . The imperfection can potentially confuse the model and harm the performance.

Therefore, given these imperfect pairs, we design an image editing model to effectively learn pertinent information, such as editing direction and preservation of untargeted subject features, from the generated pairs while simultaneously filtering out unexpected noise – specifically, small variations in identity and layout. Inspired by [22], the key design of our model is to integrate various conditions into the Stable Diffusion architecture in distinct ways. We call our model Multi-Conditioned Diffusion Model (MCDM). We will first define these conditions, and later elaborate how they help learn pertinent information from imperfect data through different injection ways. The details of the MCDM are shown in Figure 5.

Our model $\epsilon_\theta(z_t, t, \{c_s, c_{im}, c_{p_b}\})$ considers three pathways of conditional signals: (1) spatial embeddings $c_s = E(x_A)$, (2) text embeddings c_{p_b} , extracted by pretrained Stable Diffusion text encoder with target text prompt p_b as input, (3) image embeddings $c_{im} = MLP([E(x_A), CLIP_{im}(x_A)])$, where $CLIP_{im}(\cdot)$ denotes embeddings extracted from the pretrained CLIP image encoder [35]. $MLP(\cdot)$ is a multi-layer perceptron that projects image embeddings to the space of text embeddings.

To incorporate these embeddings into our model, we make modifications to the Stable Diffusion architecture as follows. (1) To prevent the imperfections in x_B from misleading the model into generating an output \hat{x}_B that alters the layout and identity in x_A , we concatenate the spatial embeddings c_s with the noisy latent z_t (input of U-Net). The resulting concatenation is then utilized as the input for the U-Net. Architecturally, the first layer of the U-Net encoder is adjusted to accommodate an additional 4 channels (for c_s), increasing the total to 8 channels. (2) c_{p_b} and c_{im} are concatenated and fed into the cross-attention layer, akin to the Stable Diffusion architecture. Functionally, c_{p_b} includes crucial information about the target domain as instructed by



Figure 6. Ablation study of design choice of MCDM, where the goal is to have the person in (a) wear a royal costume. Training from scratch (b) yields the poorest image quality due to the absence of image generation priors and text prompt interpretation. Dropping spatial embeddings (c) fails to preserve spatial layout and the person’s hairstyle. Excluding image embeddings (d) causes “over-editing” towards the target domain, compromising fidelity (e.g., the golden face in (d)). Without classifier-free guidance, less expressive edits emerge (e) (e.g., incomplete crown). In contrast, our full pipeline (f) produces the best editing results.

the text prompt, steering the output \hat{x}_B towards the desired domain B . Simultaneously, c_{im} contributes visual information derived from the input image to the cross-attention layer, offering visual guidance in the attention mechanism. This prevents \hat{x}_B from strictly adhering to the text instruction, ensuring that the output remains connected to the visual context of x_A and preventing undue deviation.

We initialize network weights with pretrained Stable Diffusion [39]. The training scheme is similar to Stable Diffusion, but with several differences: (1) we replace c_{p_b} with c_{p_a} and x_B with x_A by 5% of time. This enables the model to reconstruct input images (i.e., perform identical editing), which will be utilized during the inference phase for mask generation. (2) Inspired by [22], we implement a dropout mechanism for multiple signals for classifier-free guidance. Specifically, with a 20% probability, we drop any combination of the following: c_s , c_{im} , c_p , or even all of them.

Figure 6 illustrates the ablation of these design choices, underscoring the effectiveness of employing all conditional signals simultaneously, as previously discussed.

3.4. Mask-Guided Editing using Trained Model

After training, the standard approach for generating predictions \hat{x}_B from x_A involves denoising a random latent z_T over T iterations using trained model (with classifier-free guidance). While the generated \hat{x}_B successfully accomplishes the desired edits while preserving identity and lay-

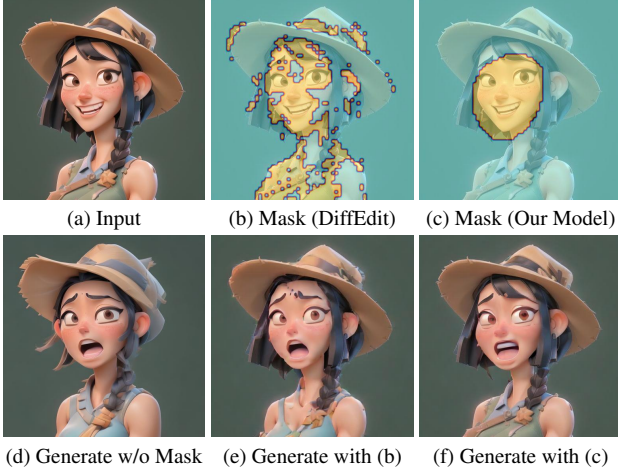


Figure 7. Comparison of mask-guided editing on cartoon expression editing (to shocked expression). Standard generation (d) alters details (e.g., patterns on hats and upper clothing) in the input image (a). Applying the mask generation strategy to our model improves the accuracy of the generated mask (c) compared to the one generated by DiffEdit (b). When guided by the mask in (c), the edited image (f) effectively preserves details (e.g., clothing) compared to the one (see (e)) guided by (b).

out, challenges may persist in retaining specific details of the subject’s features. For example, in Figure 7, an illustration of expression editing (to a shocked expression) depicts the standard generation output (d), where the hat and upper clothing patterns differ from those in the input image (a).

To enhance the preservation of these details, a mask can be derived from the trained MCDM, providing explicit guidance for the denoising process. This mask indicates areas for editing and those to be left untouched. We adapt DiffEdit [11] to automatically generate such a mask. The key difference between our and DiffEdit’s mask generation strategy is that, instead of relying on a pretrained Stable Diffusion model, we leverage our trained MCDM with its reconstruction capabilities to achieve more precise mask generation. By applying DiffEdit to our trained MCDM instead of the original Stable Diffusion model, we can achieve more precise mask generation due to MCDM’s reconstruction capability.

Figure 7 (c) shows an example of editing mask generated by our trained model, which is more accurate than the one produced by the DiffEdit used to produce pairs (Figure 7 (b)). This demonstration underscores the MCDM’s capacity to discern the types of content that should be edited, even by training on an imperfect dataset.

Once we have the mask M , at each timestep t , we calculate the mask-guided predicted noise by:

$$\hat{\epsilon} = \tilde{\epsilon}_{\theta}(z_t, t, \{c_s, c_{im}, c_{p_b}\}) \odot M + \tilde{\epsilon}_{\theta}(z_t, t, \{c_s, c_{im}, c_{p_a}\}) \odot (1 - M). \quad (3)$$

	Costume Editing Dataset			Expression Editing Dataset		
	SSIM	LPIPS	FID	SSIM	LPIPS	FID
Prompt2Prompt	0.764	0.694	83.94	0.936	0.426	33.13
pix2pix-zero	0.695	0.812	120.8	0.897	0.517	46.65
DiffEdit	0.722	0.721	93.52	0.922	0.423	32.20
SDEdit 0.8	0.681	0.766	93.17	0.914	0.461	38.59
SDEdit 0.5	0.713	0.712	68.85	0.925	0.445	38.99
SPADE	0.761	0.651	67.96	0.936	0.427	31.02
BBDM	0.776	0.676	64.17	0.937	0.432	27.26
Ours w/o Prt	0.734	0.672	84.58	0.940	0.420	28.82
Ours w/o Spt	0.767	0.665	78.38	0.735	0.430	24.56
Ours w/o Iemb	0.785	0.636	65.74	0.941	0.408	23.07
Ours w/o Mask	0.788	0.639	63.52	0.940	0.421	26.61
Ours	0.791	0.633	52.56	0.943	0.400	22.09

Table 1. Quantitative results of all tested methods, where our method outperforms all tested baselines and variants over all metrics. Please note, there are no metrics that can accurately describe the performance of models because the ground truths we used are not real and unique truths.

It implies that we denoise for target editing (using p_b) within the mask, and preserve the original image content (using p_a) outside the mask. Figure 7 (e) shows the result with mask guidance. See implementation details in supplementary.

4. Experiments

Datasets: We evaluate the performance of our pipelines in two distinct portrait editing tasks: costume editing and cartoon expression editing. For each task, we define four different editing directions for input in a specific domain. For costume editing, the input image is a realistic portrait image with everyday costume, and the output is the same person with flower, sheep, Santa Claus, or royal costume. For cartoon expression editing, the input image is a cartoon portrait with a neutral expression, while the output is the same cartoon character with four different expressions: angry, shocked, laughing, or crying. For each task, we generate a dataset of 69,900 image pairs (17475 for each editing direction) for training. The in-the-wild images for testing are from [40]. See details in supplementary.

Baselines: We choose 6 state-of-the-art image editing baselines for comparison. In particular, Prompt2Prompt [19], pix2pix-zero [34], DiffEdit [11], SDEdit [28] are training-free diffusion methods with editing direction guided by text prompt. Since SDEdit is sensitive to a strength parameter, we test two different parameters of it, namely SDEdit 0.5 and SDEdit 0.8. Larger strength produces outputs that obeys the editing directions but deviates from the input images. SPADE [33] and BBDM [26] are training-based image editing framework building on top of Generative Adversarial Networks [12] and diffusion model [13], respectively.

Real-World Applications: We showcase the practical applications of models trained on two datasets through two distinct scenarios. The first application revolves around real portrait costume editing, wherein the inputs are in-the-wild



Figure 8. In-the-Wild results comparison: existing methods either fail to apply desired edits (*e.g.*, SDEdit in first 4 rows) or struggle to figure out which region to apply the edits (*e.g.*, DiffEdit in first 4 rows). When the edits do take effect, they alter input features too much that destroy the subject’s identity (*e.g.*, facial hair in row 5 (c), arm muscle in row 6 (d)), or create significant artifacts (*e.g.*, Prompt2Prompt and BBDM). By contrast, our model can preserve input subjects’ appearance features well and achieve desired editing at high visual quality.

portrait images. As shown in top 4 rows in Figure 8, both training-based and training-free methods yield unsatisfac-



Figure 9. Comparison on validation set. In row 1 (sheep costume), the training-free baselines (b) to (d) fall short of achieving the intended edits, while the training-based methods (e) exhibit noticeable artifacts on eyes. In row 2 (angry), all baselines change the subject identity (e.g., missing glasses, wrong hair color and clothing). In contrast, our method produces high-quality editing results while preserving the identity. Note that validation set input is from generated pairs, so baseline results look better than Figure 8.

tory results; the former exhibits noticeable artifacts, while the latter often fails to align with the provided prompts.

The second application is sticker pack generation. Here, the objective is to generate a cartoon sticker pack based on an in-the-wild portrait image. To achieve this, we initially perform data augmentation, incorporating processes such as cropping and homography, on the real input image. These augmented data are then employed to train a DreamBooth [42]. Subsequently, the trained DreamBooth is utilized to generate a cartoonized portrait image of the subject, guided by a meticulously crafted text prompt. Finally, our model is applied to the cartoonized image to produce outputs featuring four distinct trained expressions. Please note, directly utilizing DreamBooth to generate images with various expressions doesn't yield satisfactory results due to the layout change and overfitting issues. As shown in Figure 8 (bottom 4 rows), training-free baselines outperform their training-based counterparts. This is because the training-based baselines are not robust enough to handle imperfect training pairs. In contrast, our method outperforms all baselines in both editing fidelity and the preservation of the subject's features, while maintaining high image quality.

User Study: We conducted a user study on two real-world applications, each with 12 examples. Participants were presented with inputs and outputs generated by DiffEdit, SDEdit 0.5, SPADE, BBDM, and our proposed pipeline, randomly shuffled. The 32 participants were asked to give a rating from 1 to 5 (higher means better) for each output. We normalized the rating of each example and user to remove the user bias. In costume editing task, our method achieves the highest average rating, surpassing DiffEdit by 3.3 times, SDEdit 0.5 by 1.8 times, SPADE by 2.1 times, and BBDM by 2.5 times. Similarly, for the expression editing, our method receives the best rating, outperforming DiffEdit by 1.7 times, SDEdit 0.5 by 1.4 times, SPADE by

2.9 times, and BBDM by 1.6 times. These results demonstrate that our method consistently produces superior visual outcomes compared with baselines in both tasks.

Comparison on Validation Set: For quantitative evaluation, we create a validation dataset for each task by generating 1,000 image pairs in two distinct ways. The first approach involves generating paired data following the same methodology described before, resulting in 100 pairs. For the second method, we adopt a different strategy aimed at introducing subjects not present in the FFHQ dataset. We exclude identity embeddings and add detailed text descriptions of individuals (generated by ChatGPT) to p , p_a , and p_b . This yields an additional 900 pairs for evaluation. We believe a more comprehensive evaluation can be conducted by combining these two types of pairs. Figure 9 and Table 1 show that our method outperforms all tested baselines.

Ablation Study: We conduct experiments to assess the effectiveness of each component of our model, resulting in four variants: (1) *Ours w/o Prt*, training our model from scratch, (2) *Ours w/o Spt*, removing spatial embeddings c_s , (3) *Ours w/o Iemb*, excluding the image embeddings c_{im} , and (4) *Ours w/o mask*, eliminating mask guidance during inference. We did not test variants without text conditions since we trained 4 editing directions using one model in the evaluation, and text conditions are used to determine which types of editing to perform at the test time. As discussed in Section 3, Table 1, Figure 6, and Figure 7 show that our final design outperforms these variants.

Limitations and Future Work: The dataset generation strategy assumes Stable Diffusion can generate images in the source and target domains, which might not always be the case. The editing performance is compromised when handling datasets with most of the pairs with significant noise, such as substantial layout and identity differences.

In the future, we will (1) move away from the constraint

of paired data and explore methods for handling unpaired data effectively, (2) reduce the required amount of training data, making the pipeline more efficient and scalable.

5. Conclusion

In this paper, we aim for portrait editing such as changing costumes and expressions while preserving the untargeted features. We introduce a novel multi-conditioned diffusion model, trained on training pairs generated by our proposed dataset generation strategy. During inference, our model produces an editing mask and uses it to further preserve details of subject features. Our results on two editing tasks demonstrates superiority over existing state-of-the-art methods both quantitatively and qualitatively.

Societal Impact: Our method should be used properly and carefully, as it could create fake images, which is an issue with image editing approaches.

Disclaimer: If any of the images belongs to you and you would like it removed from the paper, please kindly inform us and provide the relevant evidence, we will update the Arxiv paper to exclude your image.

References

- [1] Rameen Abdal, Yipeng Qin, and Peter Wonka. Image2stylegan: How to embed images into the stylegan latent space? In *Proceedings of the IEEE/CVF international conference on computer vision*, pages 4432–4441, 2019. 2
- [2] Rameen Abdal, Yipeng Qin, and Peter Wonka. Image2stylegan++: How to edit the embedded images? In *Proceedings of the IEEE/CVF conference on computer vision and pattern recognition*, pages 8296–8305, 2020. 2
- [3] Yuval Alaluf, Omer Tov, Ron Mokady, Rinon Gal, and Amit Bermano. Hyperstyle: Stylegan inversion with hypernetworks for real image editing. In *Proceedings of the IEEE/CVF Conference on Computer Vision and Pattern Recognition*, pages 18511–18521, 2022. 2
- [4] Omri Avrahami, Ohad Fried, and Dani Lischinski. Blended latent diffusion. *arXiv preprint arXiv:2206.02779*, 2022. 2
- [5] Omri Avrahami, Dani Lischinski, and Ohad Fried. Blended diffusion for text-driven editing of natural images. In *Proceedings of the IEEE/CVF Conference on Computer Vision and Pattern Recognition*, pages 18208–18218, 2022. 2
- [6] David Bau, Hendrik Strobelt, William Peebles, Jonas Wulff, Bolei Zhou, Jun-Yan Zhu, and Antonio Torralba. Semantic photo manipulation with a generative image prior. *arXiv preprint arXiv:2005.07727*, 2020. 2
- [7] Tim Brooks, Aleksander Holynski, and Alexei A. Efros. Instructpix2pix: Learning to follow image editing instructions. In *Proceedings of the IEEE/CVF Conference on Computer Vision and Pattern Recognition (CVPR)*, pages 18392–18402, 2023. 2
- [8] Tim Brooks, Aleksander Holynski, and Alexei A Efros. Instructpix2pix: Learning to follow image editing instructions. In *Proceedings of the IEEE/CVF Conference on Computer Vision and Pattern Recognition*, pages 18392–18402, 2023. 3
- [9] Tom Brown, Benjamin Mann, Nick Ryder, Melanie Subbiah, Jared D Kaplan, Prafulla Dhariwal, Arvind Neelakantan, Pranav Shyam, Girish Sastry, Amanda Askell, et al. Language models are few-shot learners. *Advances in neural information processing systems*, 33:1877–1901, 2020. 2, 3
- [10] Zhe Cao, Tomas Simon, Shih-En Wei, and Yaser Sheikh. Realtime multi-person 2d pose estimation using part affinity fields. In *Proceedings of the IEEE conference on computer vision and pattern recognition*, pages 7291–7299, 2017. 4
- [11] Guillaume Couairon, Jakob Verbeek, Holger Schwenk, and Matthieu Cord. Diffedit: Diffusion-based semantic image editing with mask guidance. *arXiv preprint arXiv:2210.11427*, 2022. 2, 6
- [12] Antonia Creswell, Tom White, Vincent Dumoulin, Kai Arulkumaran, Biswa Sengupta, and Anil A Bharath. Generative adversarial networks: An overview. *IEEE signal processing magazine*, 35(1):53–65, 2018. 6
- [13] Florinel-Alin Croitoru, Vlad Hondru, Radu Tudor Ionescu, and Mubarak Shah. Diffusion models in vision: A survey. *IEEE Transactions on Pattern Analysis and Machine Intelligence*, 2023. 6
- [14] Prafulla Dhariwal and Alexander Nichol. Diffusion models beat gans on image synthesis. *Advances in Neural Information Processing Systems*, 34:8780–8794, 2021. 2
- [15] Rinon Gal, Or Patashnik, Haggai Maron, Gal Chechik, and Daniel Cohen-Or. Stylegan-nada: Clip-guided domain adaptation of image generators. *arXiv preprint arXiv:2108.00946*, 2021. 2
- [16] Rinon Gal, Yuval Alaluf, Yuval Atzmon, Or Patashnik, Amit H. Bermano, Gal Chechik, and Daniel Cohen-Or. An image is worth one word: Personalizing text-to-image generation using textual inversion, 2022. 3
- [17] Ian Goodfellow, Jean Pouget-Abadie, Mehdi Mirza, Bing Xu, David Warde-Farley, Sherjil Ozair, Aaron Courville, and Yoshua Bengio. Generative adversarial nets. In *Advances in Neural Information Processing Systems*. Curran Associates, Inc., 2014. 2
- [18] Erik Härkönen, Aaron Hertzmann, Jaakko Lehtinen, and Sylvain Paris. Ganspace: Discovering interpretable gan controls. *Advances in neural information processing systems*, 33:9841–9850, 2020. 2
- [19] Amir Hertz, Ron Mokady, Jay Tenenbaum, Kfir Aberman, Yael Pritch, and Daniel Cohen-Or. Prompt-to-prompt image editing with cross attention control. *arXiv preprint arXiv:2208.01626*, 2022. 2, 3, 6
- [20] Jonathan Ho and Tim Salimans. Classifier-free diffusion guidance. *arXiv preprint arXiv:2207.12598*, 2022. 3
- [21] Jonathan Ho, Ajay Jain, and Pieter Abbeel. Denoising diffusion probabilistic models. *Advances in Neural Information Processing Systems*, 33:6840–6851, 2020. 2
- [22] Johanna Karras, Aleksander Holynski, Ting-Chun Wang, and Ira Kemelmacher-Shlizerman. Dreampose: Fashion image-to-video synthesis via stable diffusion. *arXiv preprint arXiv:2304.06025*, 2023. 5

- [23] Tero Karras, Samuli Laine, and Timo Aila. A style-based generator architecture for generative adversarial networks. *2019 IEEE/CVF Conference on Computer Vision and Pattern Recognition (CVPR)*, 2019. 2, 4
- [24] Tero Karras, Samuli Laine, Miika Aittala, Janne Hellsten, Jaakko Lehtinen, and Timo Aila. Analyzing and improving the image quality of StyleGAN. In *Proc. CVPR*, 2020. 2
- [25] Diederik P Kingma and Max Welling. Auto-encoding variational bayes, 2013. 2
- [26] Bo Li, Kaitao Xue, Bin Liu, and Yu-Kun Lai. Bb2m: Image-to-image translation with brownian bridge diffusion models. In *Proceedings of the IEEE/CVF Conference on Computer Vision and Pattern Recognition*, pages 1952–1961, 2023. 2, 6
- [27] Nan Liu, Shuang Li, Yilun Du, Antonio Torralba, and Joshua B Tenenbaum. Compositional visual generation with composable diffusion models. In *European Conference on Computer Vision*, pages 423–439. Springer, 2022. 3, 4
- [28] Chenlin Meng, Yutong He, Yang Song, Jiaming Song, Jiajun Wu, Jun-Yan Zhu, and Stefano Ermon. Sdedit: Guided image synthesis and editing with stochastic differential equations. *arXiv preprint arXiv:2108.01073*, 2021. 2, 6
- [29] Ron Mokady, Amir Hertz, Kfir Aberman, Yael Pritch, and Daniel Cohen-Or. Null-text inversion for editing real images using guided diffusion models. In *Proceedings of the IEEE/CVF Conference on Computer Vision and Pattern Recognition*, pages 6038–6047, 2023. 2
- [30] Chong Mou, Xintao Wang, Liangbin Xie, Yanze Wu, Jian Zhang, Zhongang Qi, Ying Shan, and Xiaoou Qie. T2i-adapter: Learning adapters to dig out more controllable ability for text-to-image diffusion models. *arXiv preprint arXiv:2302.08453*, 2023. 3
- [31] Alex Nichol, Prafulla Dhariwal, Aditya Ramesh, Pranav Shyam, Pamela Mishkin, Bob McGrew, Ilya Sutskever, and Mark Chen. Glide: Towards photorealistic image generation and editing with text-guided diffusion models. *arXiv preprint arXiv:2112.10741*, 2021. 2
- [32] Alex Nichol, Prafulla Dhariwal, Aditya Ramesh, Pranav Shyam, Pamela Mishkin, Bob McGrew, Ilya Sutskever, and Mark Chen. Glide: Towards photorealistic image generation and editing with text-guided diffusion models, 2022. 2
- [33] Taesung Park, Ming-Yu Liu, Ting-Chun Wang, and Jun-Yan Zhu. Semantic image synthesis with spatially-adaptive normalization. In *Proceedings of the IEEE Conference on Computer Vision and Pattern Recognition*, 2019. 6
- [34] Gaurav Parmar, Krishna Kumar Singh, Richard Zhang, Yijun Li, Jingwan Lu, and Jun-Yan Zhu. Zero-shot image-to-image translation. In *ACM SIGGRAPH 2023 Conference Proceedings*, pages 1–11, 2023. 2, 6
- [35] Alec Radford, Jong Wook Kim, Chris Hallacy, Aditya Ramesh, Gabriel Goh, Sandhini Agarwal, Girish Sastry, Amanda Askell, Pamela Mishkin, Jack Clark, et al. Learning transferable visual models from natural language supervision. In *International conference on machine learning*, pages 8748–8763. PMLR, 2021. 5
- [36] Aditya Ramesh, Prafulla Dhariwal, Alex Nichol, Casey Chu, and Mark Chen. Hierarchical text-conditional image generation with clip latents, 2022. 2
- [37] Danilo Jimenez Rezende and Shakir Mohamed. Variational inference with normalizing flows. *arXiv preprint arXiv:1505.05770*, 2015. 2
- [38] Daniel Roich, Ron Mokady, Amit H. Bermano, and Daniel Cohen-Or. Pivotal tuning for latent-based editing of real images. *ACM Transactions on Graphics (TOG)*, 2022. 2
- [39] Robin Rombach, Andreas Blattmann, Dominik Lorenz, Patrick Esser, and Björn Ommer. High-resolution image synthesis with latent diffusion models, 2021. 2, 3, 5
- [40] Rasmus Rothe, Radu Timofte, and Luc Van Gool. Deep expectation of real and apparent age from a single image without facial landmarks. *International Journal of Computer Vision*, 126(2-4):144–157, 2018. 6
- [41] Nataniel Ruiz, Yuanzhen Li, Varun Jampani, Yael Pritch, Michael Rubinstein, and Kfir Aberman. Dreambooth: Fine tuning text-to-image diffusion models for subject-driven generation. 2022. 3
- [42] Nataniel Ruiz, Yuanzhen Li, Varun Jampani, Yael Pritch, Michael Rubinstein, and Kfir Aberman. Dreambooth: Fine tuning text-to-image diffusion models for subject-driven generation. In *Proceedings of the IEEE/CVF Conference on Computer Vision and Pattern Recognition*, pages 22500–22510, 2023. 8
- [43] Chitwan Saharia, William Chan, Saurabh Saxena, Lala Li, Jay Whang, Emily Denton, Seyed Kamyar Seyed Ghasemipour, Raphael Gontijo-Lopes, Burcu Karagol Ayan, Tim Salimans, Jonathan Ho, David J. Fleet, and Mohammad Norouzi. Photorealistic text-to-image diffusion models with deep language understanding. In *Advances in Neural Information Processing Systems*, 2022. 2
- [44] Yujun Shen, Jinjin Gu, Xiaoou Tang, and Bolei Zhou. Interpreting the latent space of gans for semantic face editing. In *CVPR*, 2020. 2
- [45] Shelly Sheynin, Oron Ashual, Adam Polyak, Uriel Singer, Oran Gafni, Eliya Nachmani, and Yaniv Taigman. Knn-diffusion: Image generation via large-scale retrieval. *arXiv preprint arXiv:2204.02849*, 2022. 2
- [46] Jascha Sohl-Dickstein, Eric Weiss, Niru Maheswaranathan, and Surya Ganguli. Deep unsupervised learning using nonequilibrium thermodynamics. In *International Conference on Machine Learning*, pages 2256–2265. PMLR, 2015. 2
- [47] Jiaming Song, Chenlin Meng, and Stefano Ermon. Denoising diffusion implicit models. *arXiv preprint arXiv:2010.02502*, 2020. 2
- [48] Yang Song and Stefano Ermon. Generative modeling by estimating gradients of the data distribution. *Advances in Neural Information Processing Systems*, 32, 2019. 2
- [49] Yuxiang Wei, Yabo Zhang, Zhilong Ji, Jinfeng Bai, Lei Zhang, and Wangmeng Zuo. Elite: Encoding visual concepts into textual embeddings for customized text-to-image generation. *arXiv preprint arXiv:2302.13848*, 2023. 4
- [50] Zongze Wu, Dani Lischinski, and Eli Shechtman. Stylespace analysis: Disentangled controls for stylegan image generation. In *Proceedings of the IEEE/CVF Conference on Computer Vision and Pattern Recognition*, pages 12863–12872, 2021. 2

- [51] Lvmin Zhang, Anyi Rao, and Maneesh Agrawala. Adding conditional control to text-to-image diffusion models. In *Proceedings of the IEEE/CVF International Conference on Computer Vision*, pages 3836–3847, 2023. [3](#), [4](#)
- [52] Jiapeng Zhu, Yujun Shen, Deli Zhao, and Bolei Zhou. In-domain gan inversion for real image editing. In *Proceedings of European Conference on Computer Vision (ECCV)*, 2020. [2](#)
- [53] Peihao Zhu, Rameen Abdal, Yipeng Qin, John Femiani, and Peter Wonka. Improved stylegan embedding: Where are the good latents?, 2021. [2](#)

Learning Feature-Preserving Portrait Editing from Generated Pairs

Supplementary Material

1. Implementation Details

1.1. Paired Data Generation

Different pretrained Stable Diffusion models are employed for generating two datasets. The costume editing dataset is created using RealisticVision v4.0 [8]. For the cartoon expression editing dataset, fine-tuning is performed on RealisticVision v1.3 [7] using 400 images generated by the Samaritan 3D cartoon pretrained Stable Diffusion model [5]. The fine-tuned model is then used as base model to generate the cartoon expression editing dataset.

For text prompt, we set p to “the same [X] on the left and right”, where [X] corresponds to the gender (either man or woman) detected from the portrait image used to extract identity information. p_a is “a [X], [Y]”, where [Y] refers to the description of the source domain (*i.e.*, normal costume or neutral expression). p_b is “a [X], [Z]”, where [Z] is the description of the target domain. In costume editing task, [Z] are “cute flower costume”, “cute white sheep costume”, “Santa Claus costume”, or “traditional golden palace costume”. In expression editing task, [Z] are “angry”, “shocked”, “laughing”, or “crying”. In addition, we set $s'_d = 0.1$ and $s'_a = s'_b = 0.9$.

For the CLIP-based identity encoder, we train it on the FFHQ dataset [4]. As a variant of the image encoder and global mapper in [10], our architecture consists of a CLIP image encoder [6] followed by a Decoder layer [9] and a multi-layer perceptron. This identity encoder translates an input image to multiple textual word embeddings, which can be regarded as “new words” in the textual word embedding space. The resultant embeddings c_{id} have a dimension of 2×768 , which can be regarded as using two words to describe the identity. Finally, c_{id} is inserted into the position between “[X]” and its previous word in c_{p_a} . In other words, the “new words” are inserted right before “[X]”. Same operation is also performed for c_p and c_{p_b} . Images from the FFHQ dataset are utilized for identity information extraction due to the dataset’s broad diversity of identities across its entirety.

The pose image is generated using Stable Diffusion with the text prompt “a person, head shot”, resulting in 1000 candidate poses. From these candidates, one pose is randomly selected to serve as the pose condition for generating a pair.

For both datasets, the image size is set to $H = W = 512$. The denoising timestep is set to $T = 20$, and the guidance scale of the classifier-free guidance is set to 7.5. We use Stochastic Karras VE scheduler [3] for denoising.

1.2. Training Multi-Conditioned Diffusion Model

In the Multi-Conditioned Diffusion Model (MCDM), we implement $MLP(\cdot)$ following the structure described in the adapter in [2]. During training, the weights in the first layer of the U-Net related to spatial embeddings c_s are zero-initialized. For other weights, we use the same pretrained Stable Diffusion model, which was adopted for paired data generation, as the base model for initialization.

The training setup includes a batch size of 4 and a learning rate of $5e-6$. All models are trained for 200,000 steps, and the training process takes approximately 3 days on a single A100 GPU.

1.3. Mask-Guided Editing using Trained Model

During the inference phase, we set the timestep T to 20 and utilize the UniPC scheduler [11] for all tasks. Regarding the guidance scale for the classifier-free guidance, we configure $s_1 = 3$, $s_2 = 3$, and $s_3 = 5$. Here, s_1 , s_2 , and s_3 correspond to image embeddings, input embeddings, and text embeddings, respectively.

For detailed implementation of mask computation, we first add random noise to the input image x_A for 10 steps using the UniPC scheduler, resulting in z_t . Subsequently, we perform one-step denoising processes twice using the trained model, each with a distinct prompt $-p_a$ and p_b . This yields z'_{t-1} (for reconstruction) and z_{t-1} (for target editing), respectively. The distinction between z_{t-1} and z'_{t-1} is interpretable as the contrast between applying editing and not applying it. This difference is then utilized to compute the editing mask. Noteworthy is the use of p_a for reconstruction, which, as opposed to utilizing a user-defined source prompt in DiffEdit, ensures exact reconstruction and facilitates superior mask computation. Now, we can compute a binary editing mask M by $N(|z_{t-1} - z'_{t-1}|) > \lambda$, where regions with a mask value of 1 indicate areas related for editing, while those with a value of 0 remain unaltered. λ serves as a constant threshold, where a larger value results in fewer regions being marked for editing. We set λ to 0.2 and 0.35 for costume and cartoon expression editing, respectively. The operation $N(\cdot)$ denotes the normalization of the values to a range from 0 to 1, followed by a Gaussian blur with a kernel size of 5.

In practice, following the approach of DiffEdit [1], the above process is repeated with a set of 10 different z_{t-1} and z'_{t-1} (generated with different random seeds) to enhance the stability of the mask computation. This helps mitigate the potential impact of variations introduced by different random seeds during the noise addition step.

During inference, we set the timestep T to 20 and employ the UniPC scheduler [11] for all tasks. For the guidance scale of the classifier-free guidance, we set $s_1 = 3$, $s_2 = 3$, and $s_3 = 5$. We set λ to 0.2 and 0.35 for costume and cartoon expression editing, respectively.

For each task, we use the same pretrained Stable Diffusion model adopted for dataset generation as the base model for training-free baselines and initialization of our model.

2. Experiments

2.1. Datasets

For dataset generation details, please refer to Section 1.1 for details.

2.2. Real-World Applications

Figure 1 and Figure 2 show more results of costume editing task. Figure 3 and Figure 4 showcase more expression editing results. In summary, our method outperforms all baselines in both editing fidelity and the preservation of the subject’s features, while maintaining high image quality.

2.3. Comparison on Validation Set

Figure 5 and Figure 6 show the comparison between our method and all baselines on costume editing and expression editing dataset, respectively. Our method outperforms all baselines in generating high-quality editing outputs.

2.4. Ablation Study

Figure 7 shows additional results of ablation of different condition for MCDM, demonstrating the effectiveness of our final design.

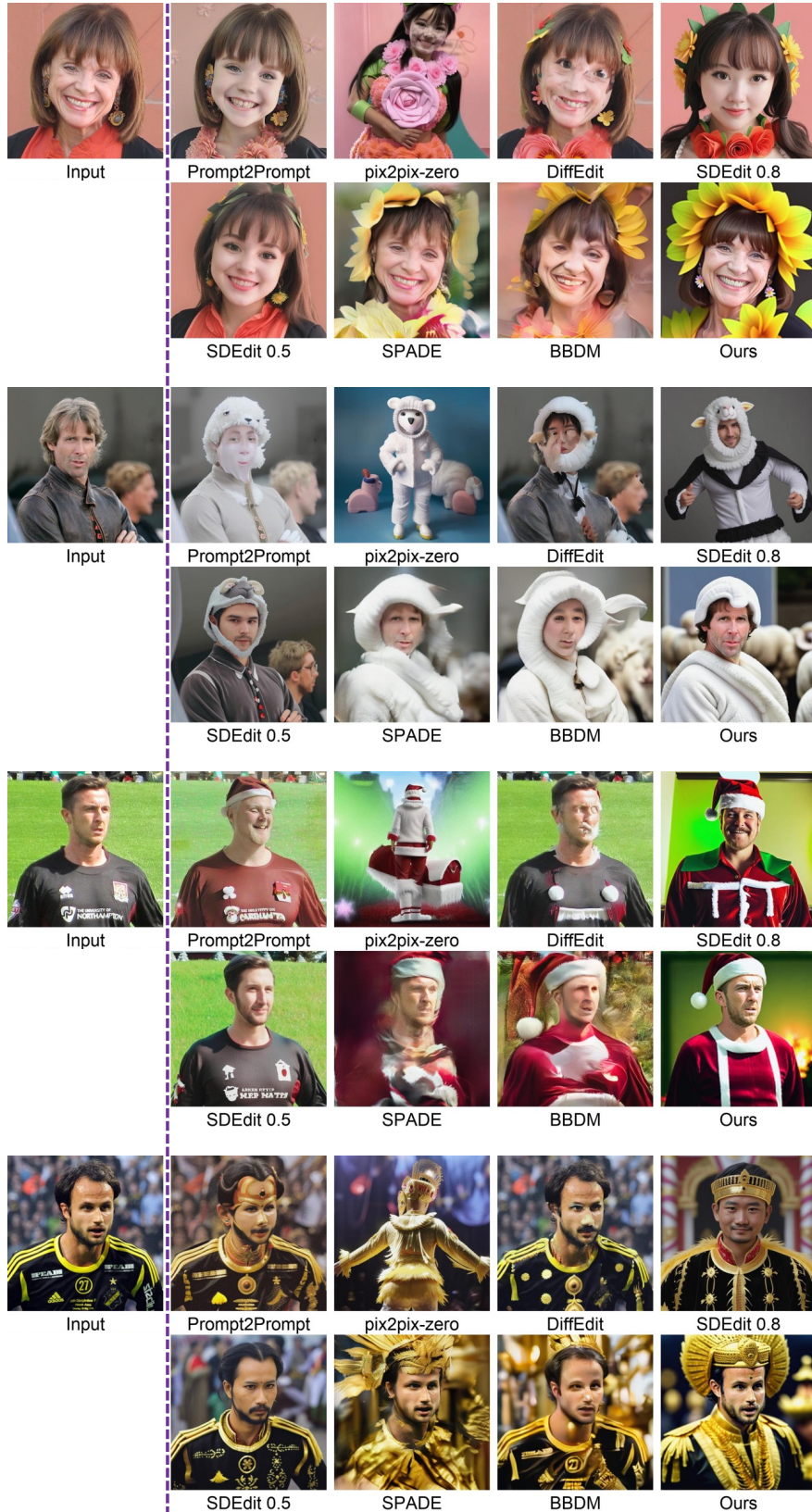


Figure 1. Costume editing comparison with baselines on in-the-wild images. Editing directions from top to bottom are to flower, sheep, Santa, and royal costume. Our method produces high-quality editing results while preserving the subject features.



Figure 2. Costume editing comparison with baselines on in-the-wild images. Editing directions from top to bottom are to flower, sheep, Santa, and royal costume. Our method produces high-quality editing results while preserving the subject features.

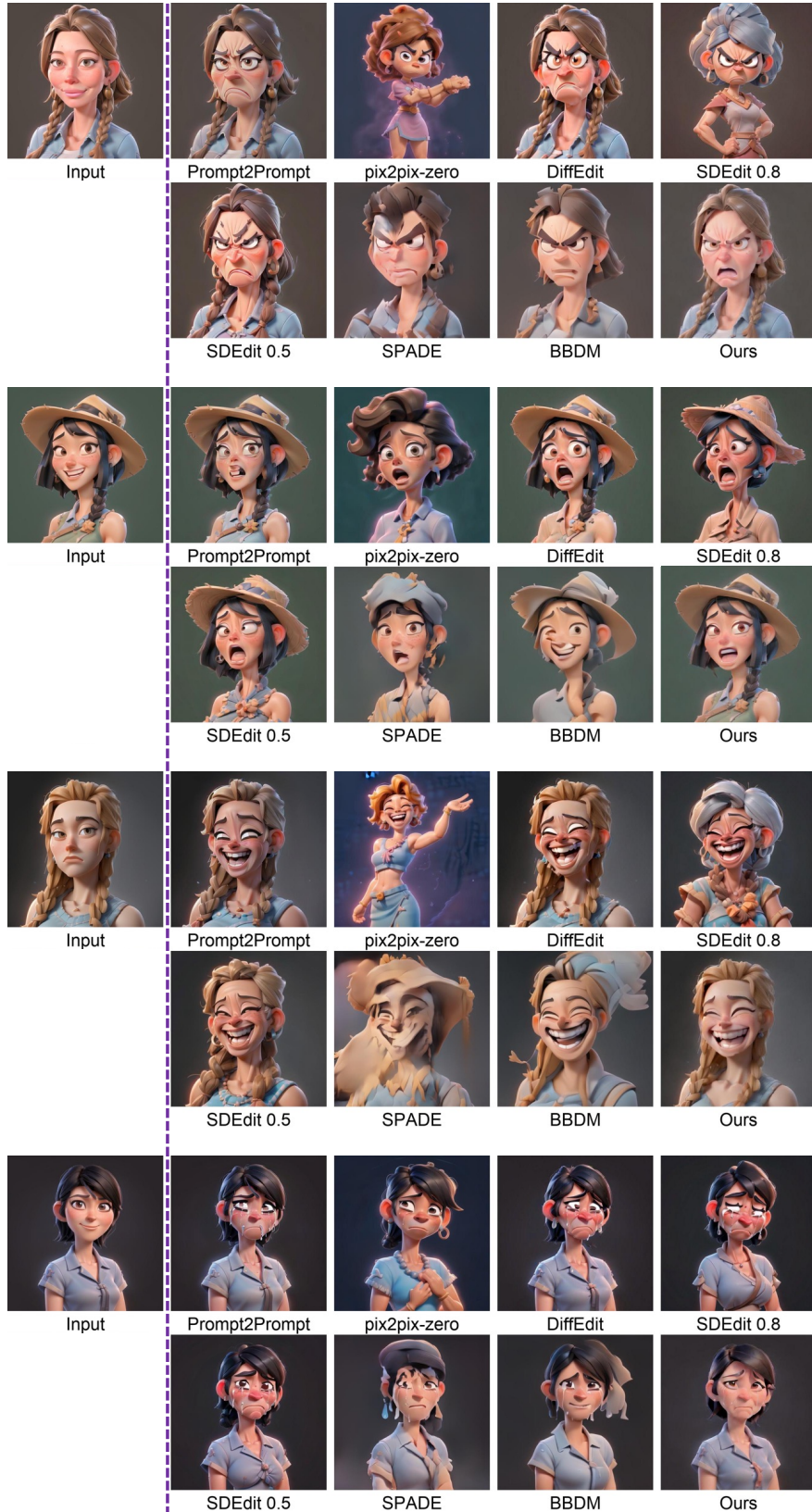


Figure 3. Expression editing comparison with baselines on cartoon input produced by DreamBooth. Editing directions from top to bottom are to angry, shocked, laughing, and crying expression. Our method produces high-quality editing results while preserving the subject features.

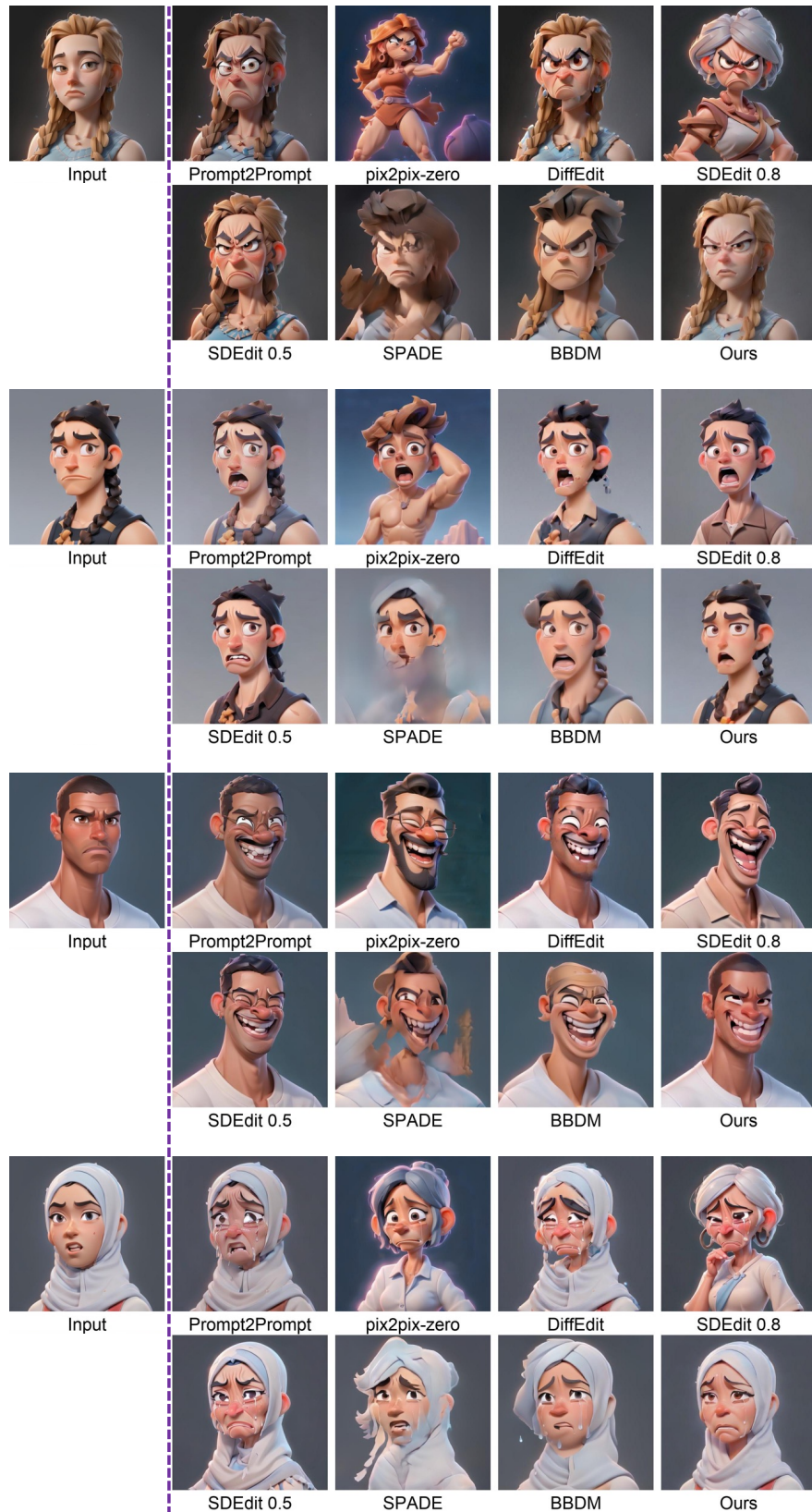


Figure 4. Expression editing comparison with baselines on cartoon input produced by DreamBooth. Editing directions from top to bottom are to angry, shocked, laughing, and crying expression. Our method produces high-quality editing results while preserving the subject features.



Figure 5. Costume editing comparison on validation set. Editing directions from top to bottom are to flower, sheep, Santa, and royal costume. Our method produces high-quality editing results while preserving the subject feature. Note that validation set input is from generated pairs, so baseline results look better than those in real-world applications.



Figure 6. Expression editing comparison on validation set. Editing directions from top to bottom are to angry, shocked, laughing, and crying expression. Our method produces high-quality editing results while preserving the subject feature. Note that validation set input is from generated pairs, so baseline results look better than those in real-world applications.



Figure 7. Ablation Study of design choice of different conditions of MCDM. Training from scratch (b) yields the poorest image quality due to the absence of image generation priors and text prompt interpretation. Dropping spatial embeddings (c) fails to preserve spatial layout. Excluding image embeddings (d) fails to learn precise editing direction, leading to artifacts in the outputs. In contrast, our full pipeline (e) produces the best editing results.

References

- [1] Guillaume Couairon, Jakob Verbeek, Holger Schwenk, and Matthieu Cord. Diffedit: Diffusion-based semantic image editing with mask guidance. *arXiv preprint arXiv:2210.11427*, 2022. [1](#)
- [2] Johanna Karras, Aleksander Holynski, Ting-Chun Wang, and Ira Kemelmacher-Shlizerman. Dreampose: Fashion image-to-video synthesis via stable diffusion. *arXiv preprint arXiv:2304.06025*, 2023. [1](#)
- [3] Tero Karras, Miika Aittala, Timo Aila, and Samuli Laine. Elucidating the design space of diffusion-based generative models. In *Proc. NeurIPS*, 2022. [1](#)
- [4] Vahid Kazemi and Josephine Sullivan. One millisecond face alignment with an ensemble of regression trees. In *Proceedings of the IEEE conference on computer vision and pattern recognition*, pages 1867–1874, 2014. [1](#)
- [5] PromptSharingSamaritan. Samaritan 3d cartoon v1.0, 2023. [1](#)
- [6] Alec Radford, Jong Wook Kim, Chris Hallacy, Aditya Ramesh, Gabriel Goh, Sandhini Agarwal, Girish Sastry, Amanda Askell, Pamela Mishkin, Jack Clark, et al. Learning transferable visual models from natural language supervision. In *International conference on machine learning*, pages 8748–8763. PMLR, 2021. [1](#)
- [7] SG_161222. Realistic vision v1.3, 2023. [1](#)
- [8] SG_161222. Realistic vision v4.0, 2023. [1](#)
- [9] Ashish Vaswani, Noam Shazeer, Niki Parmar, Jakob Uszkoreit, Llion Jones, Aidan N Gomez, Łukasz Kaiser, and Illia Polosukhin. Attention is all you need. *Advances in neural information processing systems*, 30, 2017. [1](#)
- [10] Yuxiang Wei, Yabo Zhang, Zhilong Ji, Jinfeng Bai, Lei Zhang, and Wangmeng Zuo. Elite: Encoding visual concepts into textual embeddings for customized text-to-image generation. *arXiv preprint arXiv:2302.13848*, 2023. [1](#)
- [11] Wenliang Zhao, Lujia Bai, Yongming Rao, Jie Zhou, and Jiwen Lu. Unipc: A unified predictor-corrector framework for fast sampling of diffusion models. *arXiv preprint arXiv:2302.04867*, 2023. [1](#), [2](#)